DIURNAL, SEASONAL AND SOLAR CYCLE VARIATION OF TOTAL ELECTRON CONTENT AND COMPARISON WITH IRI-2016 MODEL AT BIRNIN-KEBBI

[1,*]Aghogho Ogwala, [1]Emmanuel Olufemi Somoye, [3]Olugbenga Ogunmodimu, [1]Rasaq Adewemimo Adeniji-Adele, [1]Eugene Oghenakpobor Onori, [2]Oluwole Oyedokun

[1,*] Department of Physics, Lagos State University, Lagos, Nigeria.

[2] Department of Physics, University of Lagos, Nigeria.

[3] Department of Electrical Engineering, Manchester Metropolitan University, United Kingdom.

ABSTRACT

Total Electron Content (TEC) is an important ionospheric parameter used to monitor possible space weather impacts on satellite to ground communication and satellite navigation system. TEC is modified in the ionosphere by changing solar Extreme Ultra-Violet (EUV) radiation, geomagnetic storms, and the atmospheric waves that propagate up from the lower atmosphere. Therefore, TEC depends on local time, latitude, longitude, season, geomagnetic conditions, solar cycle activity, and condition of the troposphere. A dual frequency GPS receiver located at an equatorial station, Birnin-Kebbi in Northern Nigeria (geographic location: 12.64°N; 4.22°E; 2.68°N dip), has been used to investigate variation of TEC during the period of 2011 to 2014. We investigate the diurnal, seasonal and solar cycle dependence of observed (OBS) TEC and comparison with latest version of International Reference Ionosphere (IRI-2016) model. On a general note, diurnal variation reveals discrepancies between OBS-TEC and IRI-2016 model for all hours of the day except during the post-midnight hours. Slight post-noon peaks in the daytime maximum and post-sunset decrease and enhancement are observed in the diurnal variation of OBS-TEC of some months. On a seasonal scale, we observed that OBS-TEC values were higher in the

23 equinoxes than the solstices only in 2012. Where as in 2011, September equinox and December

24 solstice recorded higher magnitude followed by March equinox and lowest in June solstice. In

25 2013, December solstice magnitude was highest, followed by the equinoxes and lowest in June

26 solstice. In 2014, March equinox and December solstice magnitude were higher than September

27 equinox and June solstice magnitude. June solstice consistently recorded the lowest values for all

28 the years. OBS-TEC is found to increase from 2011 to 2014, thus revealing solar cycle dependence.

29 **KEYWORDS:** TEC; diurnal; seasonal; variation; solar cycle 24; IRI-2016.

30 **CORRESPONDING AUTHOR PHONE:** +234 8055650264

31 **CORRESPONDING AUTHOR E-MAIL:**ogwala02@gmail.com

33

34

35

36

37

38

39

40

41

42

43

44

45

46

47

48

INTRODUCTION

The ionosphere causes a variation in the intensity of radio signals – fading – as a result of irregularities (inhomogeneity in electron density) (Somoye, 2010; Ogwala *et al.* 2018, Ogunmodimu *et al.* 2018). Akala *et al.,* (2011) reported that the variable nature of the equatorial/ low latitude ionosphere threatens communication and navigation/ satellite systems. The equatorial/ low latitude ionosphere exhibits many unique features such as the seasonal anomaly, semi-annual anomaly, equinoctial anomaly, noon bite-out, spread-F, equatorial electrojet (EEJ), equatorial plasma bubbles (EPB) (Stankov, 2009; Maruyama *et al.,* 2004; Jee *et al.,* 2004; Codrescu *et al.,* 1999).

For many decades, scientists have been studying these ionospheric features and the role they play in trans-ionospheric electromagnetic radio wave propagation. These studies are carried out using different techniques and instruments. One of the instruments used is the GPS receiver, which provide direct measurements from satellites. Their sounding capacity extends to the topside of the ionosphere, but is affected by time and space constraints (Ciraolo and Spalla, 2002). Recently, GPS receiver is the most efficient method used to eliminate the effect of the ionosphere on radio signals. This method combines signals in different L band frequencies, L1 (1575 MHz) and L2 (1228 MHz).

Almost all space geodetic techniques transmit signals in at least two different frequencies for better accuracy (Alizadeh *et al.,* 2013). These are combined linearly and can greatly eliminate the effect of the ionosphere on radio signals. The ionospheric effect on radio signal is proportional to total electron content (TEC), which is defined as the number of electrons per square meter from satellite in space to receiver on ground is shown in equation (1).

$$TEC = \int n_e(s)ds \tag{1}$$

72   It is measured in multiples of TEC units (1 TECU = 10^{16} el/m^2). Due to the dispersive nature of

73   the ionosphere, there is a time delay between the two frequencies of a GNSS signal as it propagates

74   through the ionosphere as shown in Equation (2) as $\Delta t = t_2 - t_1$. Thus,

75    $$\Delta t = \left(\frac{40.3}{c}\right) \times \frac{TEC}{\left[\left(1/f_2^2\right) - \left(1/f_1^2\right)\right]} \qquad (2)$$

76   Where c is speed of light and f is frequency. Hence, Δt measured between the L1 and L2

77   frequencies is used to evaluate TEC along the ray path.

78   When Global Navigation Satellite System (GNSS) signals propagate through the

79   ionosphere, the carrier experiences phase advance and the code experiences a group delay due to

80   the electron density along the line of sight (LOS) from the satellite to the receiver (Bagiya *et al.,*

81   2009; Tariku, 2015). Thus, the carrier phase pseudo ranges are measured too short, and the code

82   pseudo ranges are measured too long compared to the geometric range between the satellite and

83   the receiver. This results in a range error of the positioning accuracy provided by a GPS receiver.

84   The range error due to TEC in the ionosphere varies from hundreds of meters at mid-day, during

85   high solar activity when the satellite is near the horizon of the observer, to a few meters at night

86   during low solar activity, with the satellite positioned at zenith angle (Bagiya *et al.,* 2009). By

87   measuring this delay using dual frequency GPS receivers, properties of the ionosphere can be

88   inferred and used to monitor space weather events such as GNSS, HF communications, Space

89   Based Observation Radar and Situational Awareness Radar, etc. It is documented that ionospheric

90   delay which is proportional to TEC is the highest contributor to GPS positioning error (Alizadeh

91   *et al.,* 2013; Akala *et al.,* 2013).

92   TEC in the ionosphere can also be studied using empirical ionospheric model such as the

93   International Reference Ionosphere (IRI). IRI is a joint undertaking by the Committee on Space

94 Research (COSPAR) and International Union of Radio Science (URSI) with the goal of developing

95 and improving an international standard for the parameters in earth's ionosphere (Bilitza *et al.,*

96 2014). An updated version has been developed recently to cater for lapses of previous models. IRI

97 provides the vertical TEC (VTEC) from the lower boundary (60 – 80 km) to a user-specific upper

98 boundary (Bilitza *et al.,* 2016).

99   In the past few decades, studies on the temporal and spatial variations of TEC have gained

100 popularity in the scientific community (Wu *et al.,* 2008). However, understanding the variability

101 of TEC will also go a long way in obtaining the positioning accuracy of GNSS under disturbed

102 and quiet conditions. The global distribution of TEC variations and its characteristics at all

103 latitudes, during different solar cycle phases under disturbed and quiet conditions have been

104 investigated by some researchers (Bhuyan and Borah, 2007; Maruyama *et al.,* 2004; Jee *et al.,*

105 2004).

106   Rama Rao *et al.* (2006a, b); Wanninger (1993) reported maximum day-to-day variability

107 in TEC at the Equatorial Ionization Anomaly (EIA) crest regions, increasing peak value of TEC

108 with increase in integrated equatorial electrojet (IEEJ) strength, maximum monthly average

109 diurnal variations during equinox months followed by winter months and lowest during summer

110 months. They also reported positive correlation of TEC and EEJ and the spatial variation of TEC

111 in the equatorial region. Titheridge (1974) and Langley *et al.* (2002) attributed the lower TEC

112 values during the summer seasons to low ionization density resulting from reduced O/ N_2 ratio

113 (production rates) which is a result of increased scale height. Bhuyan and Borah (2007); Komjathy

114 *et al.* (1998); Lee and Reinisch (2006) compared TEC derived from GP receivers with IRI model

115 in the equatorial/ low latitude sector and inferred that the diurnal amplitude of TEC is higher during

116 the equinoxes followed by December solstices and lowest in June solstice, i.e., observing winter

117 anomaly in seasonal variation. They further reported discrepancies between IRI model and their

118 measured values during most hours of the day at their various locations. Malik *et al.* (2016)

119 reported higher IRI values than observed maximum useable frequency (MUF) values but behaves

120 similarly diurnally and seasonally with no clear trend. Akala *et al.* (2013) on the comparison of

121 equatorial GPS-TEC observations over an African station and an American station during the

122 minimum and ascending phases of solar cycle 24 reported that seasonal VTEC values were

123 maximum and minimum during March equinox and June solstice respectively, during minimum

124 solar cycle phase at both stations. They also reported that during the ascending phase of solar cycle

125 24, minimum and maximum seasonal VTEC values were recorded during December solstice and

126 June solstice respectively. They further showed that IRI-2007 model predicted better in the

127 American sector than the African sector.

128   The aim of this paper is (i) to characterize TEC on diurnal, seasonal and solar cycle scales

129 in the Nigerian Equatorial ionosphere (ii) to compare OBS-TEC with IRI-2016 model in order to

130 find if the model underestimates or overestimates TEC values at the African longitudinal sectors.

131

132 **DATA AND METHODOLOGY**

133 **2.1 DATA**

134   The Receiver Independence Exchange (RINEX) Observation GPS data files were

135 downloaded daily from NIGNET website (www.nignet.net) and processed using Bernese software

136 and GPS TEC analysis software. The RINEX file contains 60 iteration data (i.e. in 1 minute time

137 resolution). The GPS-TEC analysis software was designed by Gopi Seemala of the Indian Institute

138 of Geomagnetism. The summary of this application is to readraw data, processes cycle slips in

139 phase data, reads satellite biases from the International GNSS services (IGS) code files (and

140   calculates them if unavailable), and calculates receiver bias, inter-channel biases for different

141   satellites in the constellation, and finally plots the VTEC values on the screen and writes the ASCII

142   output files (*CMN) for STEC and (*STD) for VTEC in the same directory of the data files. Effect

143   due to multipath is eliminated by using a minimum elevation angle of 50°.

144   Observation GPS-TEC obtained from the TEC analysis software is the slant TEC (STEC)

145   and vertical TEC (VTEC). STEC is polluted with several biases that must be eliminated to get

146   VTEC. VTEC is calculated from the daily values of STEC using equation (3).

147     $VTEC = (STEC - [b_R + b_S + b_{RX}])/S(E)$ (3)

148   Where b_R, b_S, and b_{RX} are receiver bias, satellite bias and receiver interchannel bias respectively.

149   S(E), which is the oblique factor with zenith angle, z at IPP (Ionospheric Pierce Point) is expressed

150   in equation (4).

151     $S(E) = \frac{1}{\cos(z)} = \left\{ 1 - \left(\frac{R_E \times \cos(E)}{R_E + h_S} \right)^2 \right\}^{-0.5}$ Bolaji *et al.* (2012)   (4)

152   R_E = the mean radius of the earth in km and h_S = ionospheric height from the surface of the earth.

153   According to Rama Rao *et al.,* (2006c), ionospheric shell height of approximately 350km is

154   appropriate for the equatorial/ low latitude region of the ionosphere for elevation cut off angle of

155   > 50°. This is valid in this study.

156   Hourly VTEC data obtained from these processing software are averaged to daily TEC

157   values in TEC units (1 TECU = 10^{16} el/m^2). OBS-TEC from Birnin-kebbi, on geographic Latitude

158   12.47°N and geographic Longitude 4.23°E located in Northern Nigeria, obtained during the period

159   2011 – 2014, which corresponds to the ascending (2011 – 2013) and maximum (2014) phases of

160   solar cycle 24 were compared with derived TEC obtained from International Reference Ionosphere

161   (IRI-2016) model website (https://ccmc.gsfc.nasa.gov/modelweb/models/iri2016_vitmo.php).

162   The 2016 version of IRI provides important changes and improvements on previous IRI versions

163 (Bilitza *et al.,* 2016). Solar cycle 24 is regarded as a quiet solar cycle which peaked in 2014 with

164 maximum sunspot number (103) occurring in February. Values of sunspot number, Rz, in Text

165 format were obtained from Space Physics Interactive Data Resource (SPIDR) website

166 (www.ionosonde.spidr.com) before it became unavailable. Table 1 shows the years used in this

167 study and their corresponding sunspot number, Rz.

168

169 Table I: Table of years, solar cycle phase and sunspot number, Rz [Source: Author].

Years	Solar Cycle Phase	Sunspot Number, R_z
2011	Ascending	55.7
2012	Ascending	57.6
2013	Ascending	64.7
2014	Maximum	79.6

170

171

172 **2.2 METHODOLOGY**

173 Diurnal variations of hourly OBS-TEC and hourly IRI-2016 model (NeQuick topside

174 option) were plotted using the monthly mean values of OBS-TEC and monthly mean of IRI-2016

175 model against local time (LT) on the same Figure. The corresponding percentage deviation

176 (percentage Dev or % DEV) of IRI-2016 from OBS-TEC were also analysed using the monthly

177 mean values of OBS-TEC and monthly mean values of IRI-2016 against local time (LT).

178 Percentage Dev is obtained using equations (5) below:

179 $\quad\quad\quad \%DEV = \left(\frac{OBS-IRI}{OBS}\right) \times 100 \quad\quad\quad\quad\quad\quad\quad (5)$

180   where OBS represents Observation-TEC values and IRI represents TEC derived by IRI-2016

181   model.

182   The OBS-TEC data was grouped following Onwumechilli and Ogbuehi (1964) into four

183   seasons namely: March equinox (February, March and April), June solstice (May, June and July),

184   September equinox (August, September and October) and December solstice (November,

185   December and January), in order to investigate seasonal variation. Finally, Annual variation of

186   OBS-TEC and sunspot number, Rz were also analysed by plotting mean OBS-TEC and mean Rz

187   against each month of the year.

188   **RESULT AND DISCUSSIONS**

189   Figures 1 to 4 shows the diurnal variation of OBS-TEC and IRI-2016 model in the Nigerian

190   Equatorial Ionosphere (NEI) for the years 2011 to 2014 respectively. OBS-TEC were obtained

191   from the GPS receiver installed at Birnin-Kebbi station. The diurnal variation of OBS-TEC and

192   IRI-2016 model TEC reveals the typical characteristics of an equatorial/ low latitude ionosphere.

193   Generally, the day-to-day variation of OBS-TEC have been indicated using error bar showing the

194   standard deviation from mean values. The study reveals that day-to-day variation of OBS-TEC is

195   higher during the daytime than night time for all the years. It well known fact that during the day,

196   the sun causes variations in temperature, neutral wind, electron density and electric field thereby

197   modulating the structure and evolution of the ionosphere and thermosphere (Gorney, 1990; Forbes

198   *et al.* (2006). These Figures shows a steep rise in OBS-TEC from a minimum of ~2 TECU between

199   03:00 – 05:00 LT in 2011, ~3 TECU (04:00 – 05 LT) in 2012, ~3 TECU (03:00 – 05:00 LT) in

200   2013 and 2014. OBS-TEC increased to a broad daytime maximum between 12:00 LT – 14:00 LT

201   for all years before falling to a minimum after sunset. The diurnal variation of IRI-2016 model

202   shows TEC increasing from a minimum of ~ 2 TECU in 2011, ~ 4 TECU in 2012 and 2013, and

203 ~ 5 TECU in 2014 between 03:00 – 04:00 LT for all years, to a broad daytime peak between 08:00

204 – 14:00 LT, before falling steeply to minimum before sunset. Hence the IRI-2016 model attained

205 its peak before OBS-TEC. Dabas *et al.* (2003); Somoye *et al. (*2011); Hajra *et al.* (2016); D'ujanga

206 *et al.* (2017) attributed the steep increase in TEC to solar EUV ionization and upward vertical **E** ×

207 **B** resulting from the rapid filling up of the magnetic field tube at sunrise and meridional winds

208 (Suranya *et al.,* 2015). These magnetic field tubes collapse after sunset due to low thermospheric

209 temperature and Rayleigh Taylor Instability (RTI) (Ayorinde *et al.,* 2016) giving rise to the

210 minimum TEC values after sunset. These results are similar to findings of Bolaji *et al.,* (2012),

211 Fayose *et al.,* (2012), Okoh *et al.,* (2014), Eyelade *et al.,* (2017) who have explored the NEI.

212

213
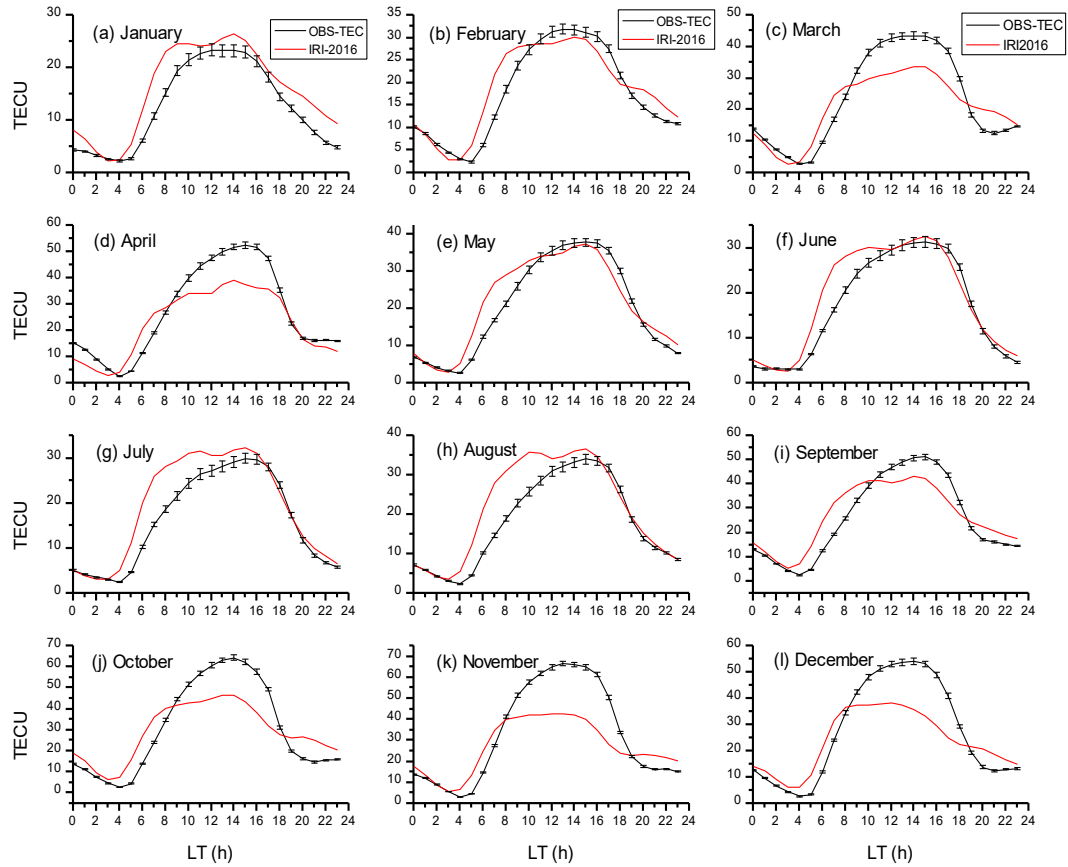
Figure 1: Diurnal variation of OBS-TEC showing error bar and IRI-2016 model of each month during January – December 2011 at Birnin-Kebbi
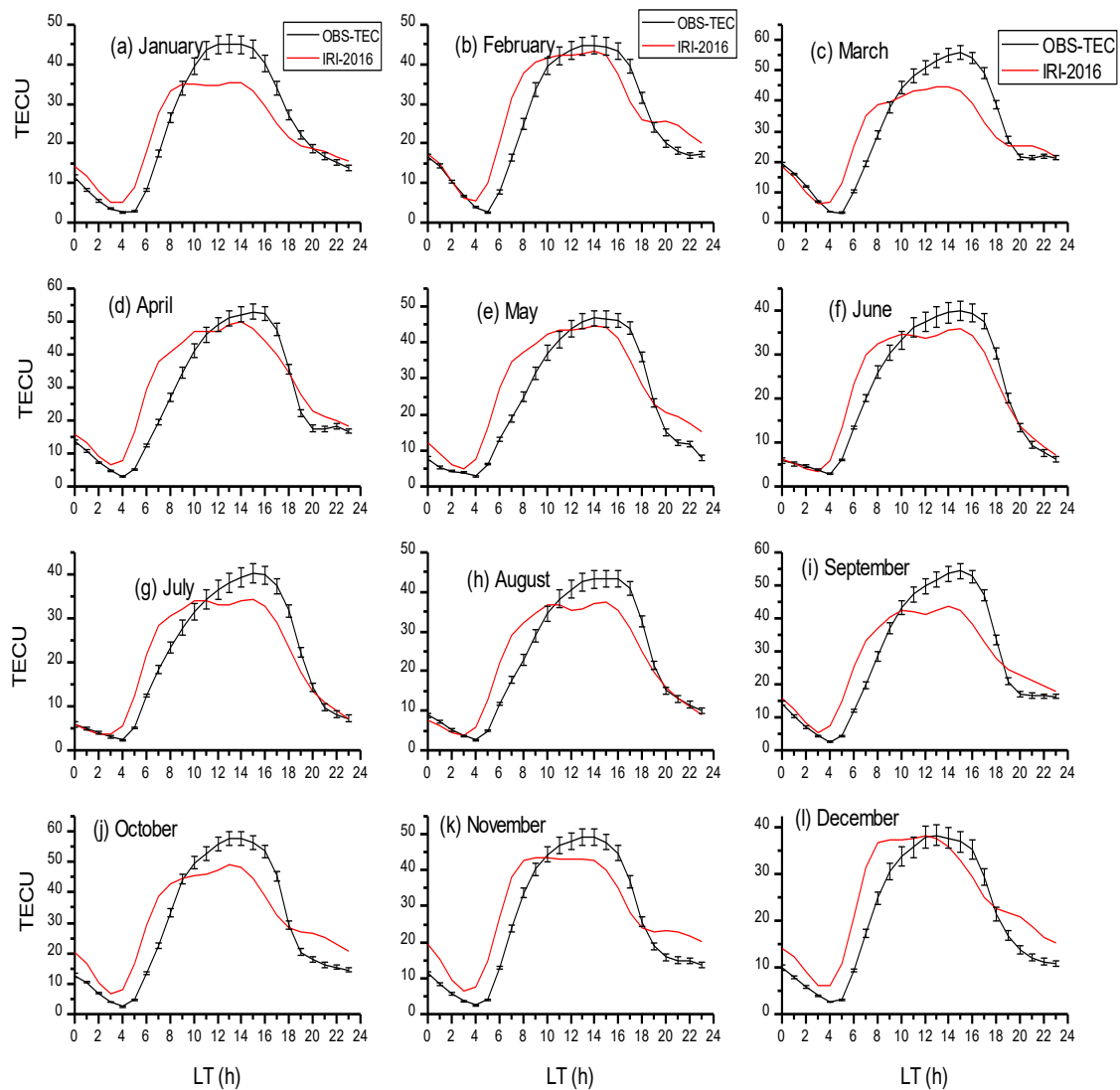
Figure 2: Same as Figure 1 for 2012.

223

224
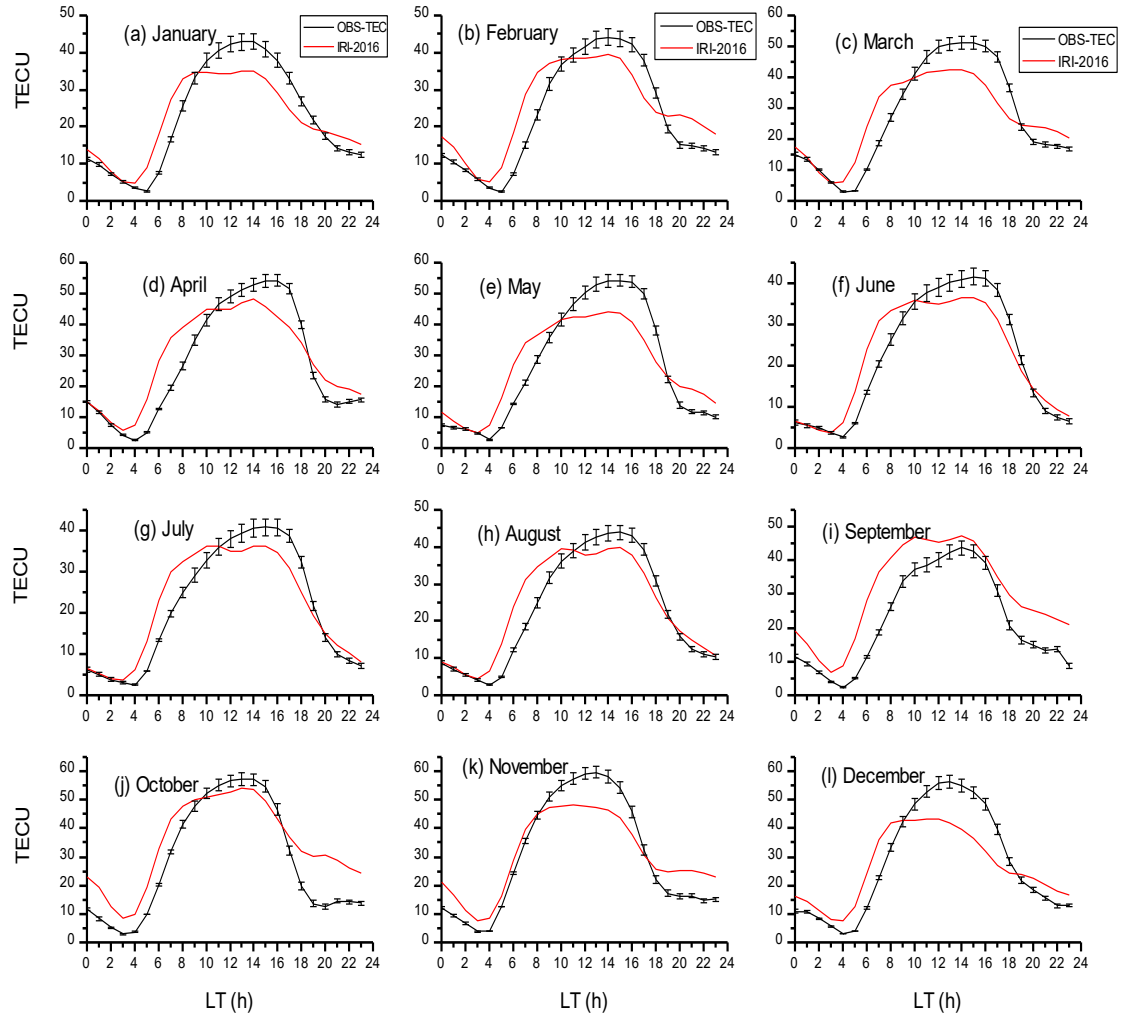
Figure 3: Same as Figure 1 for 2013.
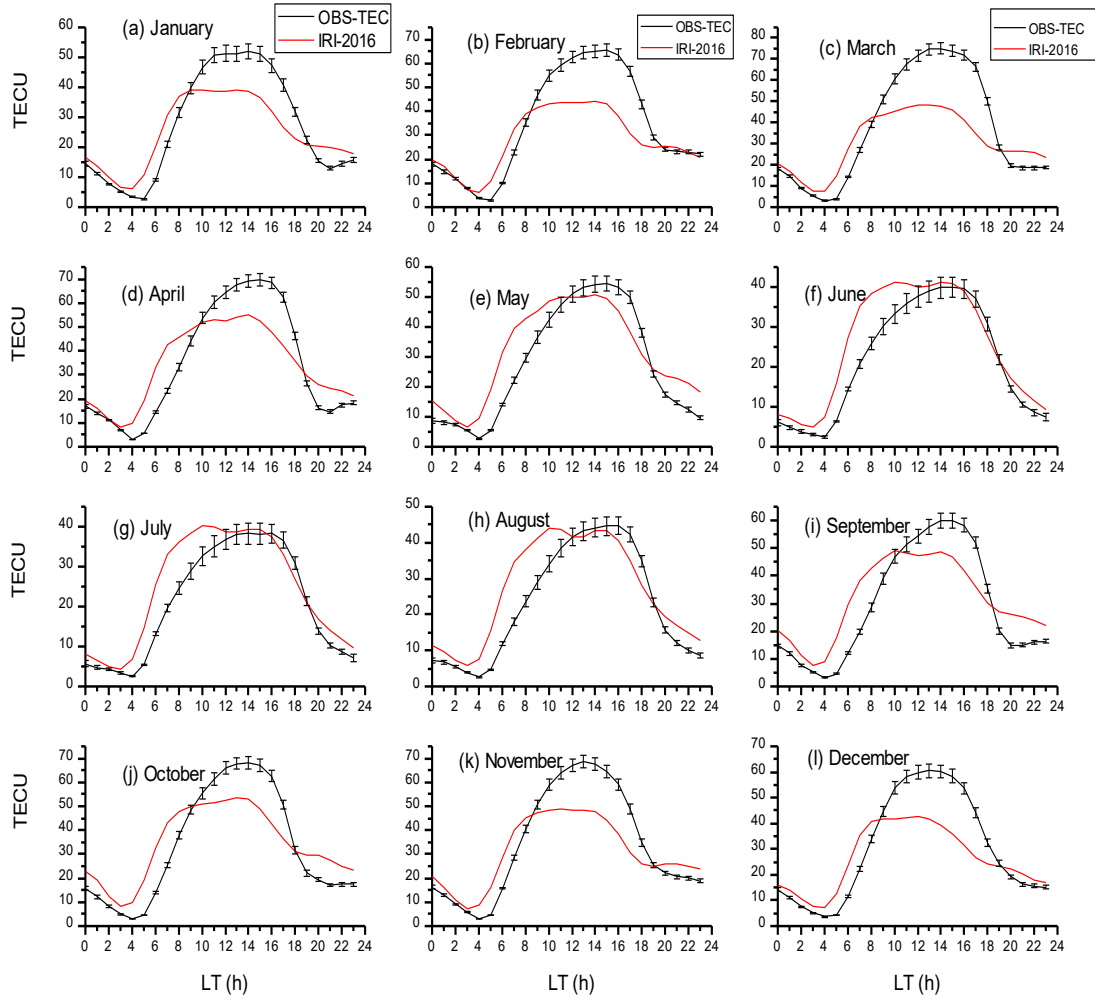
Figure 4: Same as Figure 1 for 2014.

It can be seen that OBS-TEC is much higher in 2014 with maximum value up to 70 TECU in March compared with IRI-2016 maximum of 54 TECU in the month of October, 2014. The diurnal variation reveals that the peak of OBS-TEC of majority of the months for all years shifted slightly to post-noon hours (13:00 – 14:00 LT). This type of peak shifting is peculiar to equatorial/ low latitude regions and the Polar Regions of the ionosphere and it is found to depend on the equatorial ionization anomaly and solar zenith angle respectively (Rama Rao *et al.*, 2009; D'ujanga *et al.,* 2017). Another major phenomenon seen in the diurnal variation of OBS-TEC is the post-

239 sunset decrease and slight enhancement in some months. The night time enhancement of TEC, for

240 example, March, April and October of the year 2011, March and April of the year 2012, March,

241 April, September and October of the year 2013, January, April and September of the year 2014

242 was documented by previous researchers like Rama Rao *et al.,* 2009; D'ujanga *et al.,* 2017. They

243 attributed it to the product of eastward and westward directed electric field which produces an

244 upward and downward motion of ionospheric plasma during the day and night respectively.

245   Figures 5 to 8 shows the diurnal variation of percentage deviation of IRI-2016 model from

246 OBS-TEC in the Nigerian Equatorial Ionosphere (NEI) for all years respectively. On a general

247 note, IRI-2016 model only presented suitable predictions for the post-midnight hour between 00 –

248 03hr of the day for all years. All other hours from 04 – 23hr shows some discrepancies. In some

249 months, these discrepancies lasted throughout the day for example, in the months of October,

250 November and December of 2012, October and December, 2013, and September and October of

251 2014, while in some other months these discrepancies collapsed during the pre-midnight hours (18

252 – 23hr), for example, in the months of June, July and August of 2011, June, July and August of

253 2012, June and August of 2013 and February, June and July of 2014. It is also important to mention

254 that IRI-2016 model either over estimated or under estimated TEC in the NEI especially during

255 daytime hours as shown in plots.

256

257
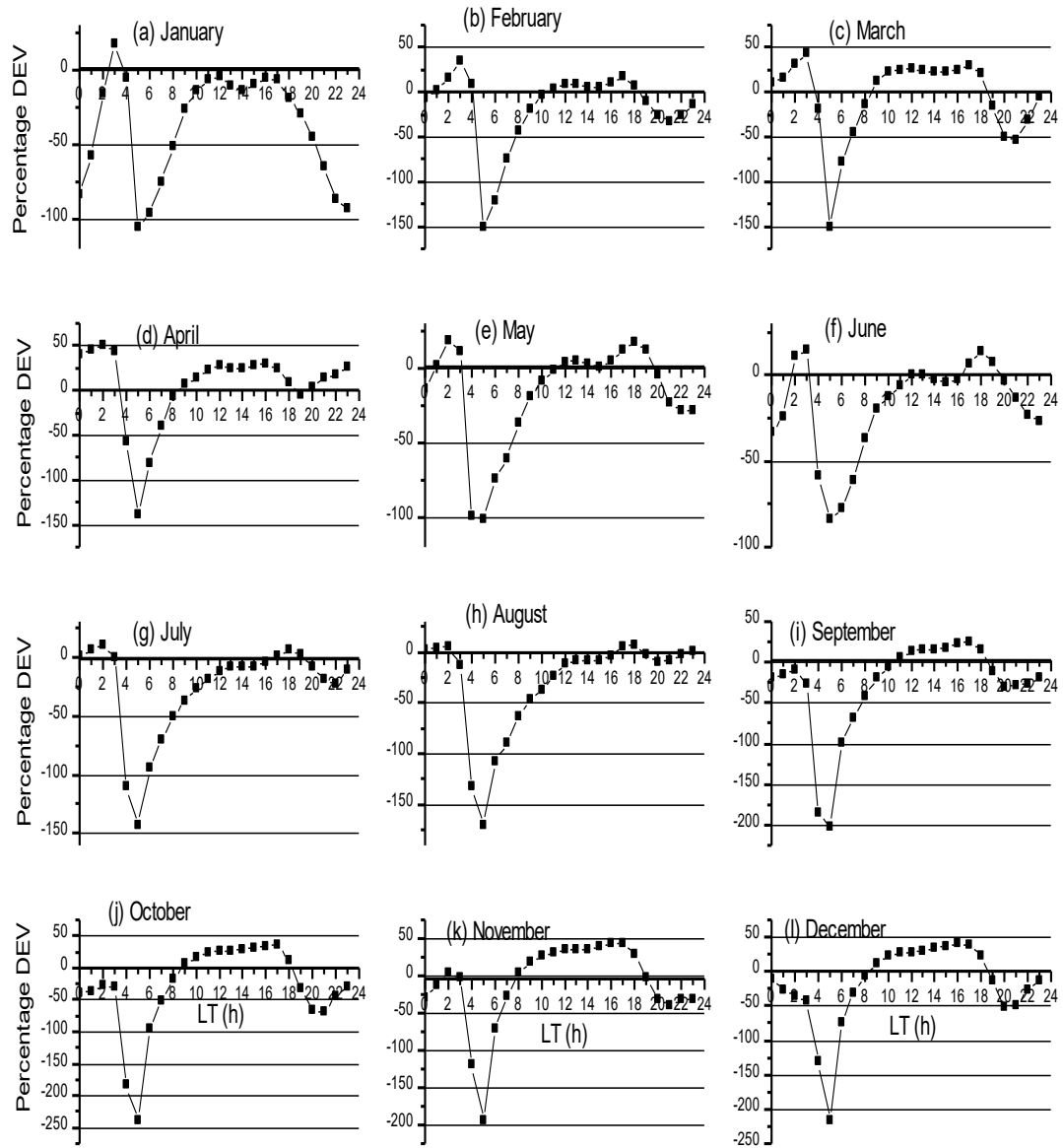
Figure 5: Percentage deviation of IRI-2016 from OBS-TEC for year 2011

258

259
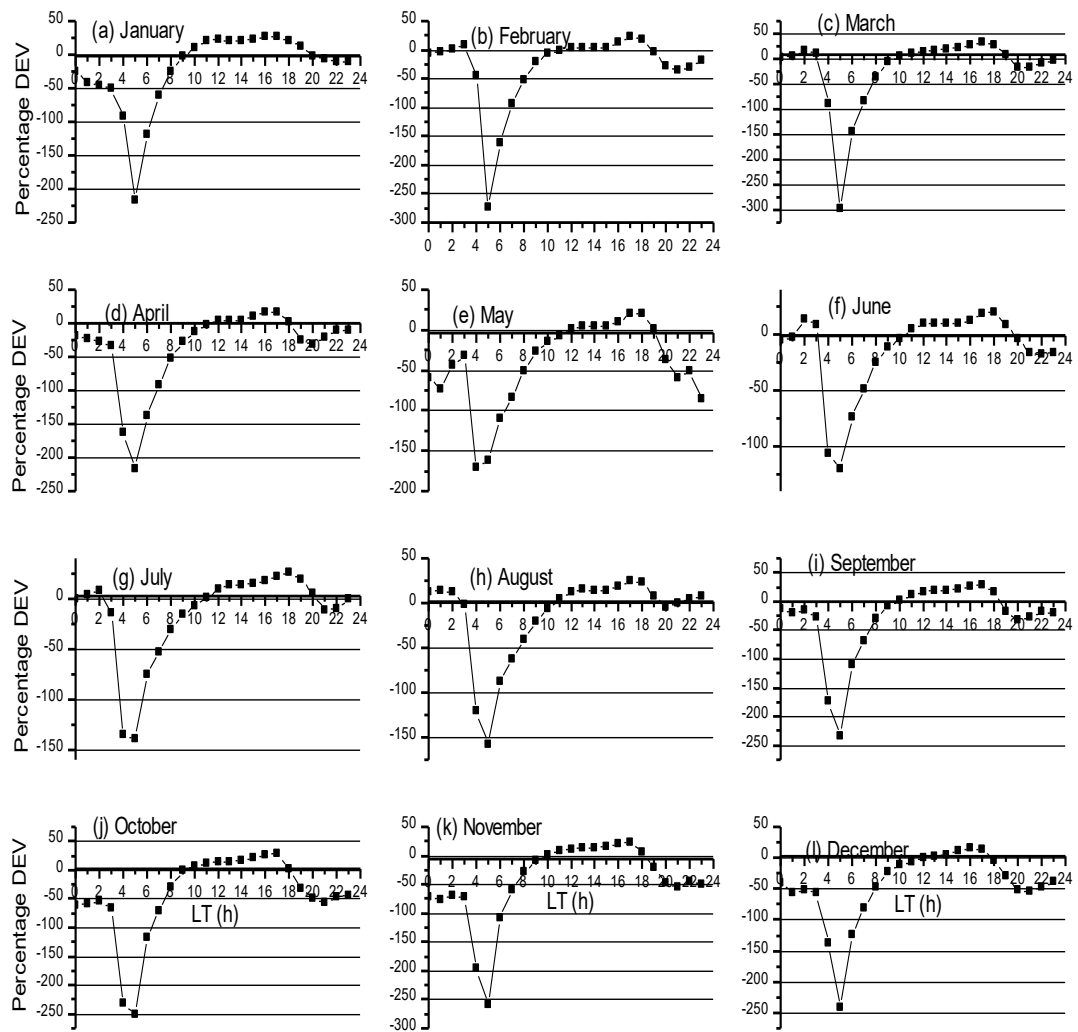
Figure 6: Percentage deviation of IRI-2016 from OBS-TEC for year 2012

260

261

262

263
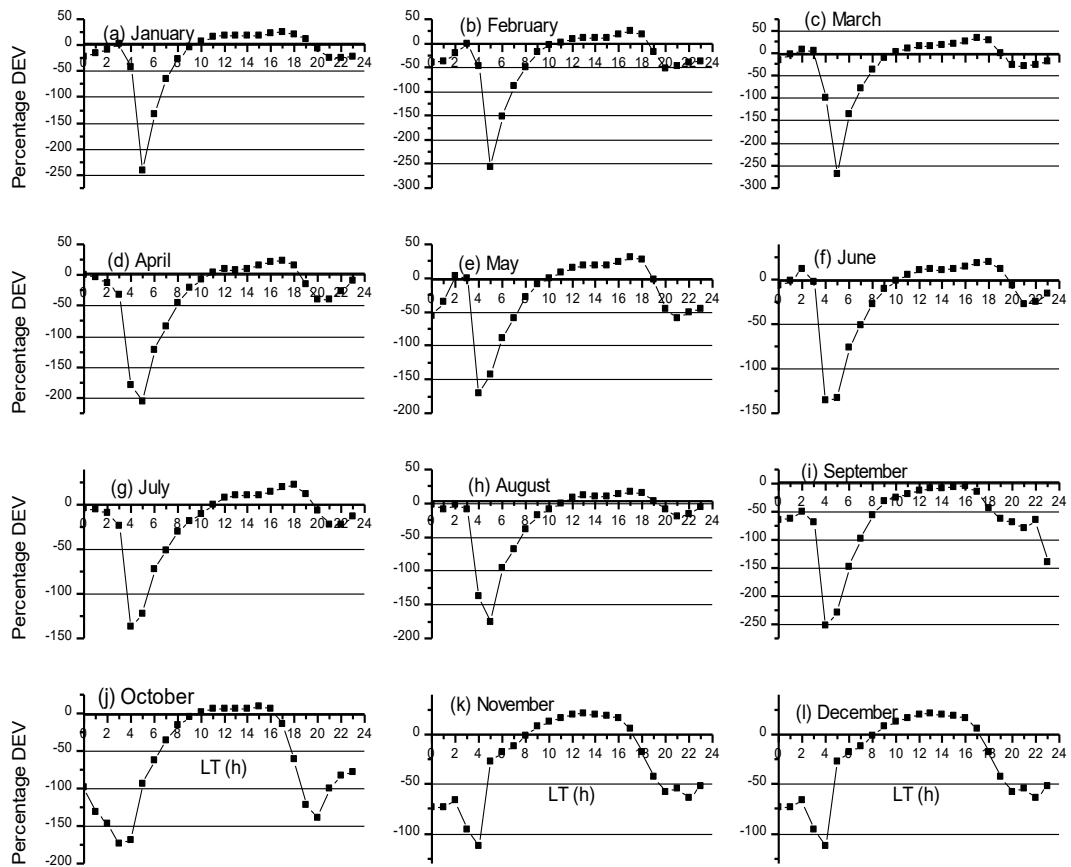
Figure 7: Percentage deviation of IRI-2016 from OBS-TEC for year 2013

264

265

266

267

268
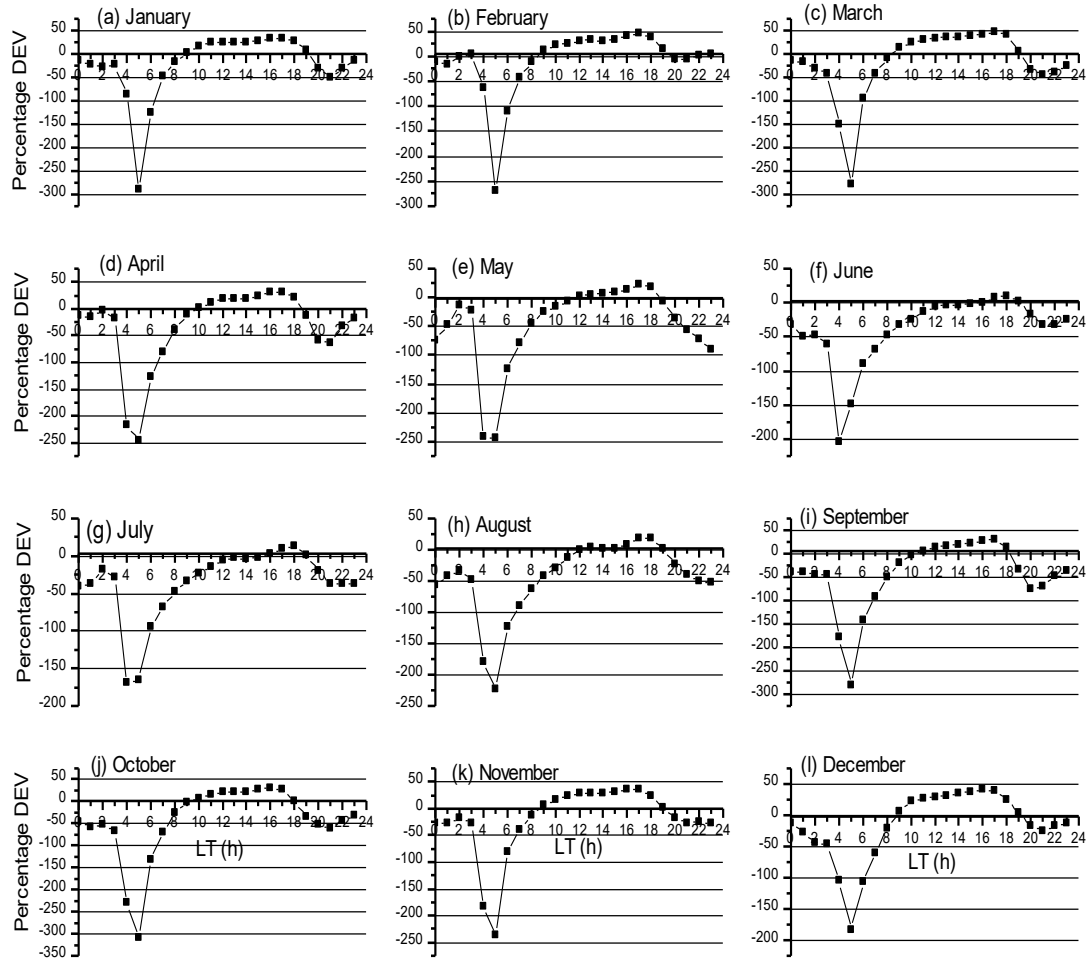
Figure 8: Percentage deviation of IRI-2016 from OBS-TEC for year 2014

269

270   The mass plots in the Figures 5 - 8 further reveal that negative percentage deviation shows

271   higher values of IRI-2016 than OBS-TEC values. The reverse is the case for positive percentage

272   deviation. Highest negative percentage deviations are seen between 04 – 05 LT for all months

273   throughout the years in this study. Highest Negative percentage deviation of ~ 300% was recorded

274   in the month of October, 2014 at 05 LT. Table II shows the summary of months with daytime

275   over- or under-estimate of IRI-2016 in the NEI.

276   Table II: Months of daytime estimate of IRI-2016 model in NEI [Source: Author]

YEAR	OVER ESTIMATE	UNDER ESTIMATE	SAME RANGE
2011	January, July, August	February – April, September - December	May - June
2012		January - December	
2013	September	January – August, October - December	
2014		January - December	

277

278   Therefore, it is clear from the Figures 1- 4, Figures 5 – 8 and Table II that IRI-2016 model

279   did not predict well in the NEI. This may be attributed to insufficient data which is as a result of

280   the sparse distribution of GPS infrastructure in this region. Our result agree with those Komjathy

281   *et al.* (1998); Lee and Reinisch (2006); Malik *et al.* (2016). Bhuyan and Borah (2007) reported

282   higher IRI TEC than their measured values at about all local time in their location. Mosert *et al.*

283   (2007) and Sethi *et al.* (2010) also reported discrepancies between of IRI TEC predictions and

284   GPS TEC during high solar activity (HSA) and low solar activity (LSA) respectively at equatorial/

285   low latitudes.

286   Figure 9 show plots the seasonal variations of OBS-TEC for the four years under

287   investigation. The change in concentration of Oxygen and molecular Nitrogen has been reported

288   to be the main cause of seasonal variation of ionospheric parameters. Seasonal variation of OBS-

289   TEC in this study depicts semi-annual variation with equinoctial maximum (~ 52 TECU) and

290   solsticial minimum (~ 44 TECU) in 2012. D'ujanga *et al.,* (2017) reported that since the sun passes

291   through the equator during the equinox, both March and September equinox experience the same

292 solar radiation. It is also a well-established fact that March 20 and September 23 are the only times

293 in the year when the solar terminator is perpendicular to the equator, giving rise to the equinoctial

294 maximum. The semi-annual variation resulting from the effect of equatorial ionization anomaly

295 (EIA) in the ionosphere has been attributed to the effect of solar zenith angle and magnetic field

296 geometry (Wu *et al.,* 2008; Rama Rao *et al.,* 2006a). Another important feature of ionospheric

297 parameters (known as equinoctial asymmetry) which is reported in the work of Bolaji *et al.,*

298 (2012); Akala *et al.,* (2013); Eyelade *et al.,* (2017); D'ujanga *et al.,* (2017); Aggarwal *et al.,* (2017),

299 is clearly seen in all years used in this work. Akala *et al.,* (2013) also reported minimum and

300 maximum seasonal VTEC values during June solstice and December solstice respectively, during

301 ascending phase of solar cycle 24. Equinoctial asymmetry is a strong phenomenon in low latitudes

302 (Aggarwal *et al.,* 2017*).* The equinoctial asymmetry has been explained in terms of the differences

303 in the meridional winds leading to changes in the neutral gas composition during the equinoxes.

304
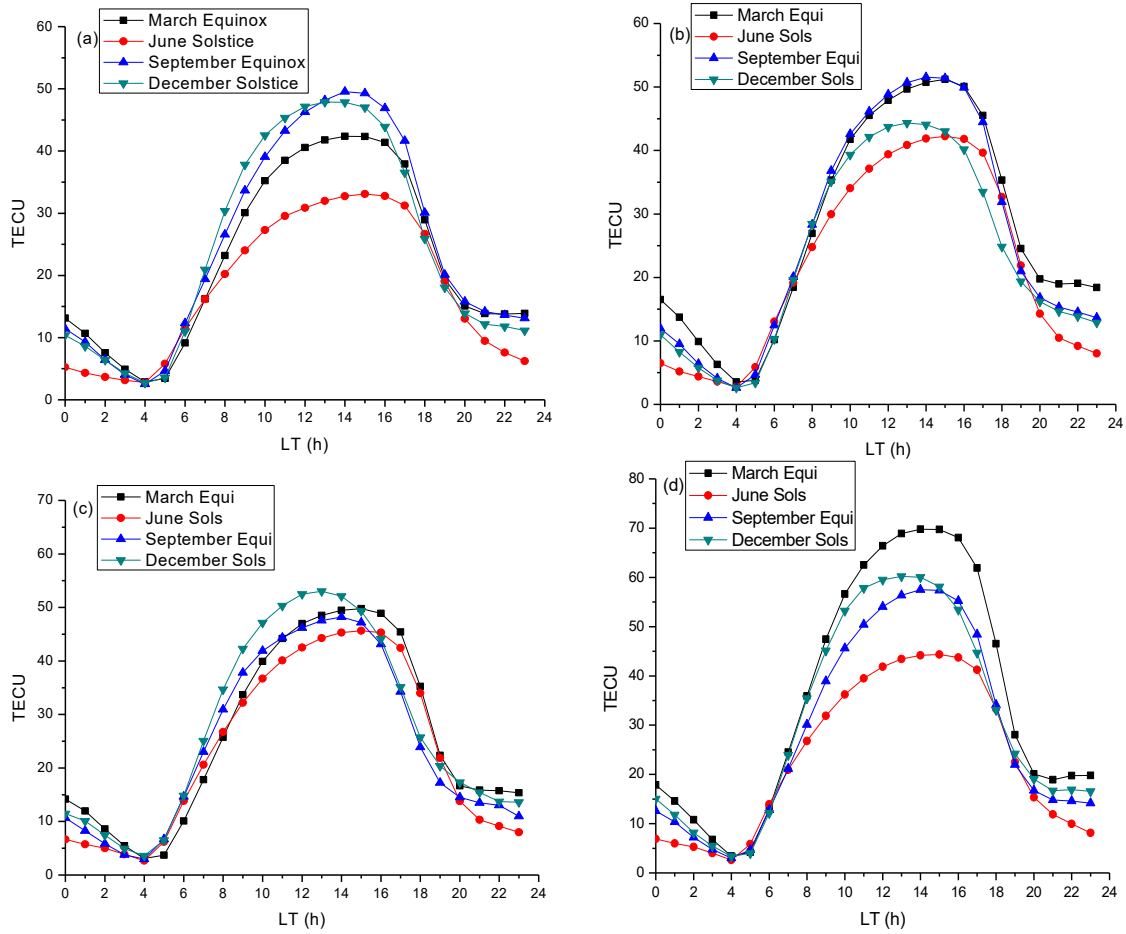
Figure 9: Seasonal variation of observed OBS-TEC during (a) 2011 (b) 2012 (c) 2013 and (d) 2014

In 2011 and 2014, the seasonal variation of OBS-TEC in the ionosphere did not follow the pattern reported by these researchers. In 2011, September equinox and December solstice recorded higher magnitude, followed by March equinox; the lowest was in June solstice. In 2013, December solstice magnitude was highest, followed by the equinoxes, March and September respectively and lowest in June solstice. This corresponds to result obtained by Akala *et al.* (2013), which they attributed to increase in ion production rate in winter season and anti-correlation between December and June Solstice pre-reversal velocity enhancement. In 2014, March equinox and December solstice magnitudes were higher than September equinox and June solstice magnitudes.

315   December solstice magnitude is found to occur between the magnitudes of the equinoxes in 2011

316   and 2014. The September equinox magnitude and March equinox magnitude are observed to

317   interchange in 2011 and 2014. Overall, June solstice magnitudes were lowest during all the years.

318   This is due to low ionization resulting from reduced production rates, i.e. O/N_2 ratio (Titheridge

319   1974). Also, for all seasons, pre-midnight (18 – 23 LT) values of TEC are higher than post-

320   midnight (00 – 05 LT) TEC values for all years. In 2011, pre- midnight TEC values are in the

321   range of 8 – 30 TECU while post-midnight TEC values ranges from 3 to 13 TECU. In 2012, pre-

322   midnight TEC values are in the range of 9 – 35 TECU while post-midnight TEC values are between

323   3 to 17 TECU. In 2013, the pre-midnight TEC values are between 9 – 35 TECU while post-

324   midnight TEC values ranges from 3 – 15 TECU. Finally in 2014, pre-midnight TEC values are

325   between 9 to 47 TECU while the post-midnight TEC ranges from 3 to 18 TECU. Furthermore, the

326   maximum OBS-TEC values in 2011 (49 TECU) and 2012 (52 TECU) were recorded in September

327   Equinox season. In 2013, OBS-TEC reached a maximum of 53 TECU in December solstice while

328   in 2014, the maximum OBS-TEC (70 TECU) was recorded in March Equinox season. This result

329   agrees in general with those of D'ujanga *et al.* (2017) who obtained higher TEC values during the

330   equinoxes than during the solstices. This same result was observed by Bagiya *et al.* (2009) that

331   TEC values are high in equinoctial months than solsticial months. Seasonal variation of TEC is

332   dependent on thermospheric neutral compositions since during the day the equator is hotter than

333   the pole. Meridional winds therefore flows from the equator towards the pole. This flow cause a

334   change in the neutral composition resulting in the decrease of the ratio of O/N_2 at the equator. The

335   decrease which is maximum at the equinox result in higher TEC values at the equinox (Bagiya *et*

336   *al.,* 2009). The corresponding annual range error (meters) of the season with maximum OBS-TEC

337   using 1 TECU variation to represent an error of 0.16m in position is summarized in Tables III.

338   Table III: Season of maximum OBS-TEC and their corresponding range error.

YEAR	SEASON OF MAXIMUM OBS-TEC	VALUE (TECU)	CORRESPONDING ERROR (m)
2011	September Equinox	49	8
2012	September Equinox	52	8
2013	December Solstice	53	8
2014	March Equinox	70	11

339

340   Figure 10 shows the comparison of the monthly OBS-TEC and sunspot number, R_z from

341   2011 – 2014, showing an increase of TEC with solar cycle. Our result is in good agreement with

342   those of Chakrabarty *et al*. (2012) and D'ujanga *et al.* (2017). The former authors reported a direct

343   solar effect on TEC while the latter authors observed that the trend in TEC follow that of solar

344   parameters. The present result also agrees with that of Rama Rao *et al.* (1985) who reported a

345   direct solar control on TEC. Ionospheric climatology especially solar activity and the equatorial

346   ionization anomaly (EIA) effects of the ionosphere provides an insight into space weather events

347   (Liu *et al.,* 2011).

348

349

350

351

352

353
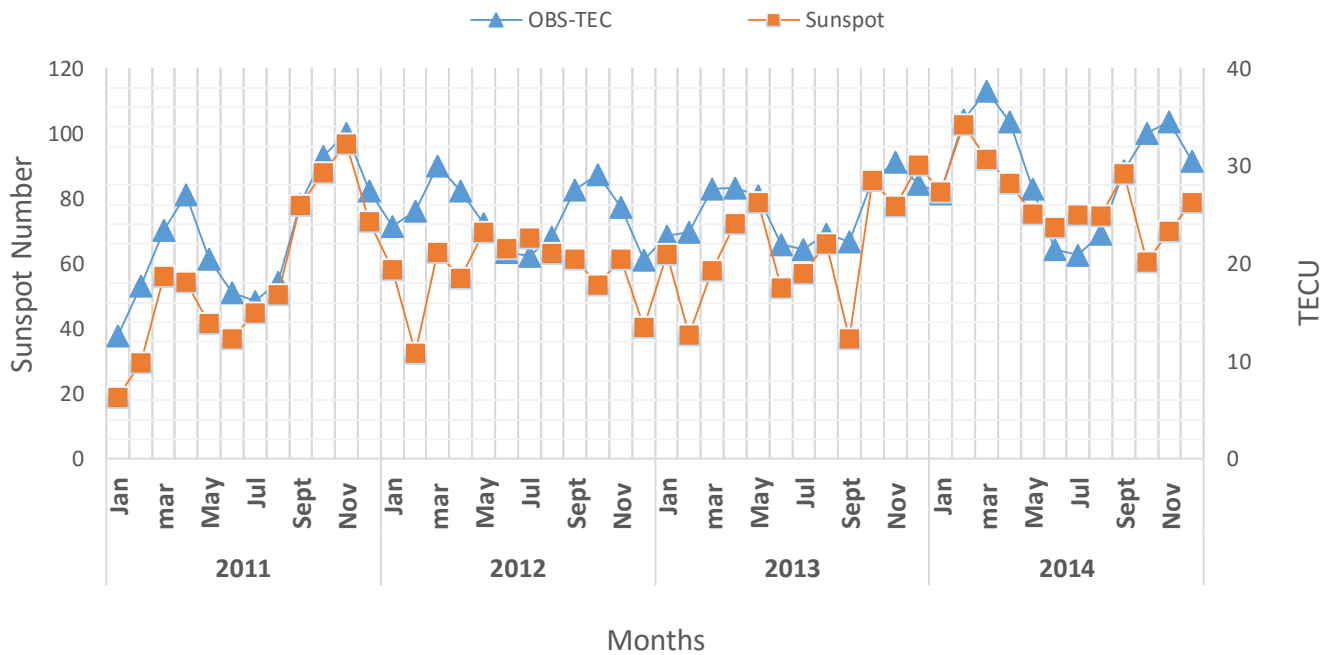
Figure 10: Annual variation of OBS-TEC and sunspot number, Rz

CONCLUSIONS

Studies on OBS-TEC and IRI-2016 model at Birnin-Kebbi in Northern Nigeria during the ascending and maximum phases of solar cycle 24 have been carried out. The result obtained reveals the following:

1. Day-to-day variations of TEC were observed to be higher during the daytime than nighttime for all the years. During the day, the sun causes variations in temperature, neutral wind, electron density and electric field in the ionosphere. The diurnal variation shows a steep rise in OBS-TEC from a minimum of ~2 TECU between 03:00 – 05:00 LT in 2011, ~3 TECU (04:00 – 05 LT) in 2012, ~3 TECU (03:00 – 05:00 LT) in 2013 and 2014. OBS-TEC increased to a broad daytime maximum between 12:00 LT – 14:00 LT for all years before falling to a minimum after sunset. Magnetic field tubes are rapidly filled up at dawn

374 resulting in the increase of extreme ultraviolet (EUV) ionization (Anderson *et al.,* 2004;

375 D'ujanga *et al.,* 2017). The diurnal variation of IRI-2016 model shows TEC rising from a

376 minimum of ~ 2 TECU in 2011, ~ 4 TECU in 2012 and 2013, and ~ 5 TECU in 2014

377 between 03:00 – 04:00 LT, to a broad daytime peak between 08:00 – 14:00 LT, before

378 falling to a minimum before sunset.

379 2. The diurnal variation reveals that the peak of OBS-TEC of some months were delayed till

380 after-noon. Post-sunset decrease and enhancement due to pre-reversal zonal electric field

381 after sunset, were also observed in the diurnal variation of OBS-TEC in some months.

382 3. On a general note, it can be concluded that IRI-2016 model and OBS-TEC show some

383 discrepancies throughout the day except during the post-midnight hours (00 – 05 LT) in

384 the NEI.

385 4. For all seasons, pre-midnight (18 – 23h) values of TEC are higher than post-midnight (00

386 – 05h) TEC values during all years. In 2011, pre- midnight TEC values are in the range of

387 8 – 30 TECU while post-midnight TEC values ranges from 3 to 13 TECU. In 2012, pre-

388 midnight TEC values are in the range of 9 – 35 TECU while post-midnight TEC values are

389 between 3 to 17 TECU. In 2013, the pre-midnight TEC values are between 9 – 35 TECU

390 while post-midnight TEC values ranges from 3 – 15 TECU. Finally in 2014, pre-midnight

391 TEC values are between 9 to 47 TECU while the post-midnight TEC ranges from 3 to 18

392 TECU.

393 5. Maximum OBS-TEC values in 2011 (49 TECU) and 2012 (52 TECU) were recorded in

394 September Equinox season. In 2013, OBS-TEC reached a maximum of 53 TECU in

395 December solstice while in 2014, the maximum OBS-TEC (70 TECU) was recorded in

396 March Equinox season. This result agrees in general with those of D'ujanga *et al.* (2017)

397   and Bagiya *et al.* (2009) who obtained higher TEC values during the equinoxes than during

398   the solstices. Seasonal variation of TEC is dependent on thermospheric neutral

399   compositions since during the day the equator is hotter than the poles.

400   6. Finally, annual variation of OBS-TEC and sunspot number, Rz reveal the strong

401   dependence of TEC on solar activity (sunspot number). Solar activity and the equatorial

402   ionization anomaly (EIA) effects of the ionosphere provides an insight into space weather

403   events. OBS-TEC and sunspot number were found to increase gradually from 2011 to

404   2014. Rama Rao *et al.* (1985) who reported a direct solar control on TEC.

405 **ACKNOWLEDGEMENT**

406 We thank the Office of the Surveyor General of the Federation (OSGoF) for making TEC data

407 available through the infrastructure www.nignet.net. We also thank Hatanaka, Y., Gopi Krishna

408 for providing TEC processing software online. Finally, we appreciate Bilitza e*t al.* (2017) for

409 making the latest version of IRI model available online.

410

411 **REFERENCES**

412 Aggarwal, M., Bardhan, A., Sharma, D.K. Equinoctial asymmetry in ionosphere over Indian

413 region during 2006 – 2013 using COSMIC measurements. Advances in Space Res., 60, 999 –

414 1014, 2017.

415 Akala, A.O., Somoye, E.O, Adeloye, A.B., Rabiu, A.B. Ionospheric f_oF_2 variability at equatorial

416 and low latitudes during high, moderate and low solar activity. Indian Journal of Radio and Space

417 Physics.Vol. 40, 124 – 129, 2011.

Akala, A.O., Seemala, G.K., Doherty, P.H., Valladares, C.E., Carrano, C.S., Espinoza, J., and Oluyo, K.S. Comparison of equatorial GPS-TEC observations over an African station and an American station during the minimum and ascending phases of solar cycle 24. Ann. Geophys., 31, 2085, 2013.

Alizadeh, M.M., Wijaya, D.D., Hobiger, T., Weber, R., Schuh, H. Ionospheric effects on microwave signals in J. Bohm and H. Schuh (eds). Atmospheric Effect in Space Geodesy. Springer atmospheric sciences. Doi: 10.1007/978-3-642-36932-2_2, © Springer-Verlag Berlin Heidelberg, 2013.

Anderson, D., Anghel, A., Chau, J., Veliz, O. Daytime vertical $\mathbf{E} \times \mathbf{B}$ drift velocities inferred from ground-based magnetometer observations at low latitudes, Space Weather, 2, S11001; doi: 10.1029/2004SW000095.

Ayorinde, T.T., Rabiu, A.B., and Amory-Mazaudier, C. Inter-hourly variability of Total Electron Content during the quiet condition over Nigeria within the Equatorial Ionization Anomaly region. J. Atmos. Solar Terr. Phys., 145, 21 – 33, 2016.

Bagiya, M.S., Joshi, H.P., Iyer, K.N., Aggarwal, M., Ravin-dran, S., and Pathan, B.M. TEC variations during low solar activity period (2005 – 2007) near the Equatorial Ionization Anomaly Crest region in India. Ann Geophys., 27, 1047 – 1057, 2009.

Bhuyan, P.K. and Borah, R.R. TEC derived from GPS network in India and comparison with the IRI. Advances in Space Res., 39, 830 – 840, 2007.

Bilitza, D., Altadill, D., Zhang, Y., Mertens, C., Truhlik, V., Richards, P., McKinnell, L.A., Reinisch, B. International reference ionosphere 2012 – A model of international collaboration. J. Space Weather Space Clim., 4, 1 – 12, doi: 10.1002/201JA018009, 2014.

440 Bilitza, D., Altadill, D., Truhlik, V., Shubin, V., Galkin, I., Reinisch, B., and Huang, X.

441 International reference ionosphere 2016: from ionospheric climate to real-time weather

442 predictions. Space weather, 15, 418 – 429, doi: 10.1002/20165SW001593, 2016.

443 Bolaji, O. S., Adeniyi, J.O., Radicella, S.M., and Doherty, P.H. Variability of total electron content

444 over an equatorial West African station during low solar activity. Radio Sci., 47, RS1001, doi:

445 10.1029/2011RS004812, 2012.

446 Charkrabarty, D., Bagiya, M.S., Thampi, S.V., Iyer, K.N. Solar EUV flux (0.1 – 50 nm), $F_{10.7}$ cm

447 flux, sunspot number and total electron content in the crest region of the ionization anomaly during

448 the deep minimum between solar cycle 23 and 24. Indian Radio and Space Phys., 41, 110 – 120,

449 2012.

450 Ciraolo, L., and Spalla, P. TEC analysis of IRI simulated data. Adv. Space Res., 29, 6, 959 – 966,

451 2002.

452 Codrescu, M. V., Palo, S. E., Zhang, X., Fuller-Rowell, T. J., Poppe, C. TEC climatology derived

453 from TOPEX/POSEIDON measurements, Journal of Atmospheric Solution, 61, 281-298, 1999.

454 Dabas, R.S., Singh, L., Lakshmi, D.R., Subramanyam, P., Chopra, P., Garg, S.C. Evolution and

455 dynamics of equatorial plasma bubbles: relationships to $\mathbf{E} \times \mathbf{B}$ drifts, post-sunset total electron

456 content enhancements, and equatorial electrojet strength. Radio Sci., 38, doi:

457 10.1029/2001RS002586, 2003.

458 D'ujanga, F.M., Opio, P. Twinomugisha, F. Variation of total electron content with solar activity

459 during the ascending phase of solar cycle 24 observed at Makerere University, Kampala. Space

460 Weather: Longitude and Hemispheric Dependences and Lower Atmosphere Forcing, Geophysical

461 Monograph 220, First Edition. Edited by Timothy Fuller-Rowell, Endawoke Yizengaw, Patricia

462   H. Doherty, and Sunanda Basu. © 2017 American Geophysical Union. Published 2017 by John

463   Wiley & Sons, Inc., 2017.

464   Eyelade, V.A., Adewale, A.O., Akala, A.O., Bolaji, O.S. and Rabiu, A.B. Studying the variability

465   in the diurnal and seasonal variations in GPS TEC over Nigeria. Ann. Geophys., 35, 701 – 710,

466   2017.

467   Fayose, R.S., Rabiu, B., Oladosu, O., Groves, K. Variation of total electron content (TEC) and

468   their effect on GNSS over Akure. Nigeria, Applied Physics Research, 4, 2, 2012.

469   Forbes, J.M., Bruinsma, S., Lemoine, F.G. Solar rotation effects in the thermospheres of Mars

470   and Earth. Science, 312, 1366–1368, 2006.

471   Gorney, D. J. Solar cycle effects on the near-earth space environment. Rev Geophys, 28, 315–

472   336, 1990.

473   Hajra, R., Chakraborty, S.K., Tsurutani, B.T., DasGupta, A., Echer, E., Brum, C.G.M., Gonzalez,

474   W.D., Sobral, H.A. An empirical model of ionospheric total electron content (TEC) near the crest

475   of the equatorial ionization anomaly (EIA). J. Space Weather Space Clim., 6, A29, doi:

476   10.1051/swsc/2016023, 2016.

477   Liu, L., Wang, W., Chen, Y., Le, H. solar activity effects on the ionosphere: A brief review. Space

478   Physics and Space Weather Geophysics. Chinese science Bulletin. 56, 12, 1202 – 1211, 2011.

479   Jee, G., Schunk, R. W., Scherliess, L. Analysis of TEC data from the TOPEX/Poseidon mission,

480   Journal of Geophysical Research, 109, A01301, doi:10.1029/2003JA010058, 2004.

481   Komjathy, A., Langley, R., Bilitza, D. ingesting GPS-derived data into the IRI for single frequency

482   radar altimeter ionospheric delay corrections. Adv. Space Res., 22, 6, 793 – 802, 1998.

483 Langley, R., Fedrizzi, M., Paula, E., Santos, M., Komjathy, A. Mapping the low latitude

484 ionosphere with GPS. GPS World, 13, 2, 41 – 46, 2002.

485 Lee, C.C. and Reinisch, B.W. Quiet condition hmF2, NmF2 and Bo variations at Jicamarca and

486 comparison with IRI-2001 during solar maximum. J. Atmos. Solar Terr. Phys., 68, 2138 – 2146,

487 2006.

488 Maruyama, T., Ma, G., and Nakamura, M. Signature of TEC storm on 6 November 2001 derived

489 from dense GPS receiver network and ionosonde chain over Japan. Journal of Geophysical

490 Research, 109, A10302, doi: 10.1029/2004JA010451, 2004.

491 Mosert, M., Gende, M., Brunini, C., Ezquer, R. and Altadill, D. Comparisons of IRI TEC with

492 GPS and Digisonde measurements at Ebro. Advances in Space Res., 39, 841 – 847, 2007.

493 Okoh, D., Lee-Anne McKinnell, L., Cilliers, P., Okere, B., Okonkwo, C., Rabiu, A.B. IRI-VTEC

494 versus GPS-vTEC for Nigerian SCINDA GPS stations. Advances in Space Research,

495 http://dx.doi.org/10.1016/j.asr.2014.06.037, 2014.

496 Ogunmodimu, O., Rogers, N.C., Falayi, E., Bolaji, S. Solar Flare induced cosmic noise absorption,

497 NRIAG Journal of Astronomy and Geophysics. 7, 1, 31-39, 2018.

498 Ogwala, A., Somoye, E.O., Oyedokun, O., Adeniji-Adele, R.A., Onori, E.O., Ogungbe, A.S.,

499 Ogabi, C.O., Adejo, O., Oluyo, K.S., Sode, A.T. Analyses of Total Electron Content over Northern

500 and Southern Nigeria. J. Res. and Review in Sci., 21 – 27, 2018.

501 Onwumechilli, C.A., and Ogbuehi, P.O. Journal Atmos. Terr. Phys., 26, 894, 1964.

502 Rama Rao, P.V.S., Niranjan, K., Rama Rao, B.V., Rama Rao, B.V.P.S., Prasad, D.S.V.V.D. Proc.

503 URSI/ IPS Conference on the ionosphere and Radio wave Propagation. Sydney, Australia, 1985.

504 Rama Rao, P.V.S., Krishna, S.G., Prasad, J.V., Prasad, S.N.V.S., Prasad, D.S.V.V.D., Niranjan,

505 K. Geomagnetic storm effects on GPS based navigation. Ann. Geophys., 27, 2101 – 2110, 2009.

506 Rama Rao, P.V.S., Krishna, S.G., Niranjan, K., Prasad, D.S.V.V.D. Study of temporal and spatial

507 characteristics of L-band scintillation over the Indian low-latitude region and their possible effects

508 on GPS navigation. Ann. Geophys., 24, 1567 – 1580, 2006a.

509 Rama Rao, P.V.S., Krishna, S.G.,Niranjan, K., Prasad, D.S.V.V.D. Temporal and spatial

510 variations in TEC using simultaneous measurements from indian GPS network of receivers during

511 low solar activity period of 2004 – 2005. Ann. Geophys., 24, 3279 – 3292, 2006b.

512 Rama Rao, P.V.S., Niranjan, K., Prasad, D.S.V.V.D., Krishna, S.G., Uma, G. On the validity of

513 the ionospheric pierce point (IPP) altitude of 350km in the Indian equatorial and low-latitude

514 sector. Ann. Geophys., 24, 2159 – 2168, 2006c.

515 Sethi, N. K., Pandey, V. K., Mahajan, K. K. Comparative study of TEC with IRI model for solar

516 minimum period at low latitude. Advances in Space Research, 27, 45 – 48, 2010.

517 Suranya, P.L., Prasad, D.S.V.V.D., Niranjan, K., Rama Rao, P.S.V. Short term variability in foF2

518 and TEC over low latitude stations in the Indian sector. Indian J. of Radio and Space Phys., 44, 14

519 – 27, 2015.

520 Somoye, E.O. Diurnal and seasonal variation of fading rates of E- and F-region echoes during IGY

521 and IQSY at the equatorial station of Ibadan. Indian Journal of Radio and space Physics, 38, 194

522 – 202, 2010.

523 Somoye, E.O., Akala, A.O., Ogwala, A. Day-to-day variability of h'F and foF2 during some solar

524 cycle epochs. Journal Atmos. Solar Terr. Physics, 73, 1915 – 1922, 2011.

525   Stankov, S. M. Trans-ionospheric GPS signal delay gradients observed over mid-latitude Europe.

526   Advances in Space Research, 43, 1314–1324, 2009.

527   Tariku, Y.A. Pattern of GPS-TEC variability over low-latitude regions (African sector) during the

528   deep solar minimum (2008 to 2009) and solar maximum (2012 to 2013) phases. Earth, Planets,

529   and space. 67, 35, 2015.

530   Titheridge, J.E. Changes in atmospheric composition inferred from ionospheric production rates.

531   J. Atmos. Terr. Phys., 36, 1249 – 1257, 1974.

532   Wanninger, L. Effects of the equatorial ionosphere on GPS. GPS World, 2, 48, 1993.

533   Wu, C.C., Liou, K., Shan, S.J., Tseng, C.L. Variation of ionospheric total electron content in

534   Taiwan region of the equatorial anomaly from 1994 – 2003. Adv. Space Res., 41, 611 – 616, 2008.

535

536